

# A Concurrent Dual-Band Low Noise Amplifier for GNSS Receivers

M. Safari\*, M. Eghtesadi\* and M. R. Mosavi\*(C.A.)

**Abstract:** In this paper, a new design of concurrent dual-band Low Noise Amplifier (LNA) for multi-band single-channel Global Navigation Satellite System (GNSS) receivers is proposed. This new structure is able to operate concurrently at frequency of 1.2 and 1.57 GHz. Parallel and series resonance parts are employed in the input matching in order to achieve concurrent performance. With respect to used pseudo-differential structure, LNA is basically a single-ended-to-differential conversion and it consequently has no need to balun. In addition, an inductively degenerated cascode approach is employed to have better simultaneous matching and Noise Figure (NF). Simulations are performed with TSMC 0.18  $\mu\text{m}$  technology in ADS software. Results analysis present that LNA achieves input matchings of -11.024 and -13.131 dB, NFs of 2.315 and 2.333 dB, gains of 26.926 and 27.576 dB,  $P_{-1\text{dB}}$  of -15.3 and -13 dBm, IIP3 of -0.9 and 2.2 dBm at 1.2 and 1.57 GHz, respectively. Besides, LNA consumes 8.32 mA DC current from a 1.8 V supply voltage.

**Keywords:** Concurrent Dual-Band, GNSS, Impedance Matching, LNA, Noise Figure.

## 1 Introduction

GNSS provides electronic equipment with positioning, velocity and time information [1]. It is noticeable that the system utilizes satellites for RF signal transmissions.

Global Positioning System (GPS), which was advanced by US military department, is now the only useable navigation system throughout the world. GPS satellites as a part of GPS system are always trying to send out three different kind of signals (L1, L2 and L5) during moving in the space [2]. Broadcasting radio signals over wireless channels through GPS satellites enables GPS receivers to figure out the precise location, speed and time in different weather conditions [3]. But the sensitivity and accuracy of GPS system to find the positions is really affected by special environment around the receivers. In fact, not only working in wooded areas, jamming and multi-path environment can decay the accuracy of GPS system, but also received signals in buildings or under tunnels also might be inaccurate. Therefore, employing the simple GPS system with single band reception is not able to provide appropriate availability and navigation accuracy [4].

On the other hand, GNSS systems, including

GLONASS by Russia, Galileo by European Union and Compass by china, have not reached out GPS capability in terms of global coverage yet [5]. Apart from coverage, however, low sensitivity of GNSS systems has always obtained users complaints [6]. In order to increase the sensitivity and precision, GNSS receivers have to support more than one GNSS system simultaneously [7, 8]. Since GNSS systems work with two frequency bands (1.2 and 1.5 GHz), they should have supported both of the bands. The GNSS signals specifications are listed in Table 1. Dual-band receivers are divided into two main groups [9]: 1) concurrent: simultaneous dual-band support and 2) non-concurrent: non-simultaneous dual-band support.

Due to more electronics components in non-concurrent's high power consumption structures, it is not good candidate in modern electronics systems [10]. Concurrent dual-band receivers can support two bands through two channels [4, 11-17] or one channel [18,19]. Utilizing two channels receivers not only increases the power consumption, but it also expands the size and used area. Therefore, they are not considered as an efficient approach, but receiving two bands from just one channel can optimize power consumption and area consumption. As an alternative in two bands structures, using only one channel can optimize the power and area consumption and improves the system performance. That's why this kind of structures has been selected as a case study.

---

Iranian Journal of Electrical & Electronic Engineering, 2016.

Paper received 25 December 2015 and accepted 18 May 2016.

\* The Authors are with the Department of Electrical Engineering, Iran University of Science and Technology, Narmak, Tehran, Iran.

E-mails: maryam\_safari@elec.iust.ac.ir, M\_Eghtesadi@elec.iust.ac.ir and M\_Mosavi@iust.ac.ir.

**Table 1** List of GNSS signals

System	Band	Carrier Freq. (MHz)	BW (MHz)	Power (dBW)	Access Technique
GPS	L1 C/A	1575.42	2.046	-158.5	CDMA
	L2 C	1227.6	2.046	-164.5	
	L5	1176.45	20.46	-157.9	
GLONASS	L1	1602	-	-161	FDMA
	L2	1246	-	-167	
Galileo	E1	1575.42	4.092	-157	CDMA
	E5a	1176.45	20.46	-155	
	E5b	1207.14	20.46	-155	
BD-2	B1	1561.098	4.092	-163	CDMA
	B2	1207.14	20.46	-163	

In order to concurrent dual-band structure, we need a special frequency plan. There are some reasons which make the Low Noise Amplifier (LNA) one of the most important blocks of concurrent dual-band receiver, because of lower power in RF signal compared to thermal noise, have high gain and low Noise Figure (NF) in LNA causes designing process to be complicated. Also, LNA should support two frequency bands in one channel. Since LNA block plays an important role in receiver's structure, other parameters such as linearity, and power consumption should be optimized. As a result, LNA design is considered to be extremely important step in concurrent dual-band receivers design.

This paper is organized as followed. Section 2 describes the architecture of proposed concurrent dual-band LNA. Section 3 would discuss simulation results. It also goes through a full analysis of simulation results and comparison with previous works. Section 4 gives a thorough conclusion of this paper.

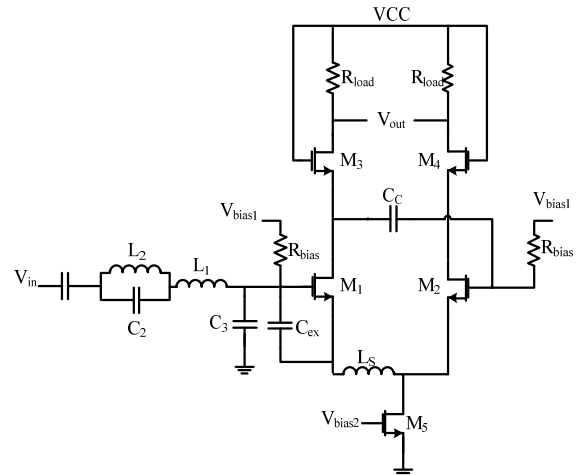
## 2 LNA Architecture

Fig. 1 represents an overview of proposed concurrent dual-band LNA. The small-signal equivalent circuit of Fig. 1 is delineated in the Appendix. LNA structure is pseudo-differential amplifier with inductively degenerated common source topology.

The basic concept of the proposed circuit is relied on the differential amplifier with differential outputs and inputs as shown in Fig. 2. In order to eliminate the input balun, the mentioned structure can be modified to pseudo-differential.

The most important advantage of using single-ended-to-differential conversion is front-end protection, particularly in high common mode interference situation. In addition, the more switching rate at the back end of the receiver makes this structure more effective. Other advantages are mentioned as follow: 1) decrease the feedthrough of the local oscillator at the mixer output and 2) removing off-chip balun because of LNA single input.

In more details, different parameters of the proposed case study are discussed below.



**Fig. 1** Schematic of the proposed LNA.

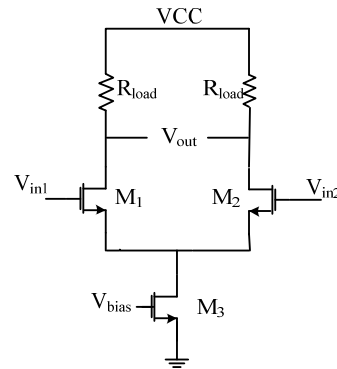


**Fig. 2** Differential amplifier.

### 2.1 Concurrent Dual-Band Matching

Matching is a significant part of LNA designing process in order to achieve the maximum power transmission. Different parts of the input matching circuit are depicted in Fig. 1. As can be seen in this figure,  $L_2$ ,  $C_2$  are placed in the parallel resonant part as well as  $L_1$ ,  $L_s$ , and  $C_t$  ( $C_t = C_{ex} \parallel C_{gs}$ ) are employed in series resonant part. These two resonance parts provide simultaneous matching for two required frequency bands (1.2 and 1.57 GHz in this case).

Besides, in order to realize the input matching, the input impedance should be equal to conjugation of the source impedance:

$$Z_{opt} = Z_s^* \quad (1)$$

where  $Z_s^*$  is source impedance conjugate and  $Z_{opt}$  is optimal noise impedance.

To attain the small NF, the optimum noise source impedance can be determined as follow [20]:

$$\text{Re}[Z_{opt}] = \frac{\alpha \sqrt{\frac{\delta}{5\gamma} (1 - |c|^2)}}{\omega C_{gs1} \left\{ \frac{\alpha^2 \delta}{5\gamma} (1 - |c|^2) + \left( \frac{C_t}{C_{gs1}} + \alpha |c| \sqrt{\frac{\delta}{5\gamma}} \right)^2 \right\}} = R_s \quad (2)$$

where  $\alpha$  is a constant value.  $\delta$  and  $\gamma$  are gate induced noise and channel noise coefficients, respectively, and  $c$  is the correlation coefficient between the gate induced noise and channel noise.

$$\text{Im}[Z_{\text{opt}}] = j\omega \left[ \frac{L_2}{1 - \omega^2 L_2 C_2} + L_1 + L_s - \frac{1}{\omega^2 C_t} \right] = 0 \quad (3)$$

in which  $C_t$  is the equivalent of parallel  $C_{\text{ex}}$  and  $C_{\text{gs}}$  capacitors (capacitors between gate and source of M1) providing simultaneous noise and input matching for two bands.

Based on Eq. (2) for one frequency band and by substituting  $\omega$  for 1.57 GHz,  $C_{\text{ex}1}$  can be solved. In order to achieve input matching, following equation should be satisfied:

$$Z_{\text{in}} = Z_s^* \quad (4)$$

$$\text{Re}[Z_{\text{in}}] = \frac{g_m L_s}{C_t} = R_s \quad (5)$$

$$\text{Im}[Z_{\text{in}}] = j\omega \left[ \frac{L_2}{1 - \omega^2 L_2 C_2} + L_1 + L_s - \frac{1}{\omega^2 C_t} \right] = 0 \quad (6)$$

where  $g_m$  is transconductance of M1.  $g_m$  is derived from bias current, which has been calculated by power constraint technique. Since Eq. (3) and Eq. (6) are equivalent, both of them can be used to determine  $L_1$ ,  $L_2$  and  $C_t$ . However, solving the equation for both frequencies (1.2 and 1.57 GHz) will result in several values for these parameters. Final determination should satisfy both parallel and series resonant parts.

## 2.2 Gain

The gain is adversely affected by the load, which is resistive in the proposed structure (Fig. 1). This makes the resonance frequencies solely dependent on the matching network. Finding this resistance is a major challenge in LNA design because of some intrinsic limitations. The upper bound is limited by the gain and the lower bound is limited by the resistance power and voltage. The proposed design has determined this resistance, so the voltage dropping is lower than cascode transistor's threshold. Therefore transistors are constantly in saturated region.

Gain can be determined from:

$$\text{Gain} = 2Q_{\text{in}} g_m R_L \quad (7)$$

where  $Q_{\text{in}}$  is the quality factor of input matching network. Because of the differential structure, the gain in Eq. (7) is multiplied by 2. It means that it should be increased by 6 dB.

## 2.3 Compensation Capacitor

Pseudo-differential structure, which is used in this paper, is not thoroughly symmetrical. Therefore, a capacitor is required to equalize the current of both sides in terms of magnitude and phase. This capacitor, which is called compensation capacitor, injects current

to the right side and compensates the difference of both sides. The injected current can be expressed:

$$i_{\text{injected}} = g_{m2} V_{G2} \quad (8)$$

$$V_{G2} = \frac{C_c}{C_c + C_{\text{gs}2}} V_{D1} \quad (9)$$

$$V_{D1} = -\frac{Q_{\text{in}} g_{m1} V_s}{g_{m3}} \quad (10)$$

So that,  $V_{G2}$  is the gate voltage of M2,  $V_{D1}$  is the drain voltage of M1 and  $V_s$  is the source voltage.

From the above equations, the value of the  $C_c$  is determined so that, the extra current compensates the decreasing current at the half right of the circuit. In order to analyze the effect of  $C_c$  in the proposed circuit, the drain current is depicted in the Figs. 3 and 4.

## 3 Simulation Results

A new design of concurrent dual-band LNA which is able to operate at both required frequency bands (1.2 and 1.57 GHz) is proposed in this study. Simulations are performed in TSMC 0.18  $\mu\text{m}$  technology in ADS software.

To analysis of the input matching, the S11 parameter is demonstrated in Fig. 5. As can be seen in this figure, S11 can reach -11.024 and -13.131 dB in 1.2 and 1.57 GHz, respectively. In addition, It is clear that matching occurs simultaneously only in the mentioned operating frequencies and never happens in other frequencies.

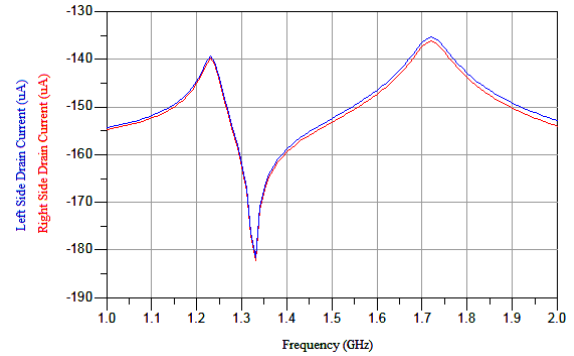


Fig. 3 Drain currents without  $C_c$

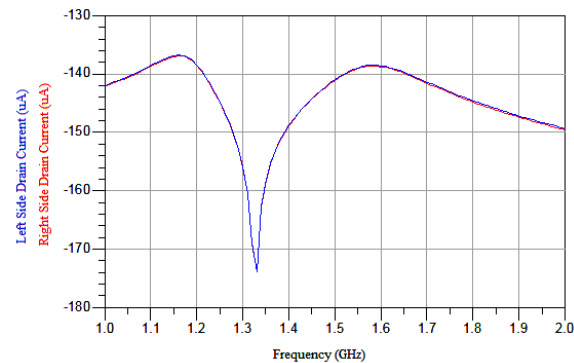
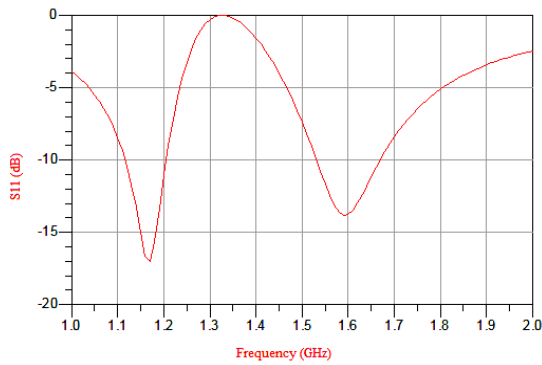


Fig. 4 Drain currents with  $C_c$



**Fig. 5** Simulation result of S11 parameter.

Fig. 6 shows the gain curve for suggested LNA. Regarding the matching in two frequency bands, the gain has reached a reasonable amount. The gain values for 1.2 and 1.57 GHz are 26.926 and 27.576 dB, respectively. Due to less source negative feedback effect in higher frequencies, gain is higher in 1.57 GHz. As shown in this figure, the gain curve has formed a notch shape. This notch has occurred because of input mismatching and causes the attenuation of image and unwanted signals between these frequencies. Attenuation amount in these frequencies is about 18 dB.

To more investigation, the effect of cascode approach on miller effect and isolation is perceptible from Fig. 7. According to this figure, it is evident that S12 values in 1.2 and 1.57 GHz are -39.557 and -39.089 dB, respectively.

Fig. 8 depicts the NF diagram of a proposed LNA. Designed LNA has reached a much reliable amount in both frequency bands concurrently. Based on Fig. 8, NF, is 2.315 and 2.333 dB in 1.2 and 1.57 GHz, respectively. As can be seen in this figure, although the NF value between these two frequency bands reaches 25 dB, the gain attenuation is approximately 18 dB (Fig. 6) that prevents the unwanted signals to pass through circuit. Therefore, the circuit performance cannot be affected by high NF between this frequency ranges.

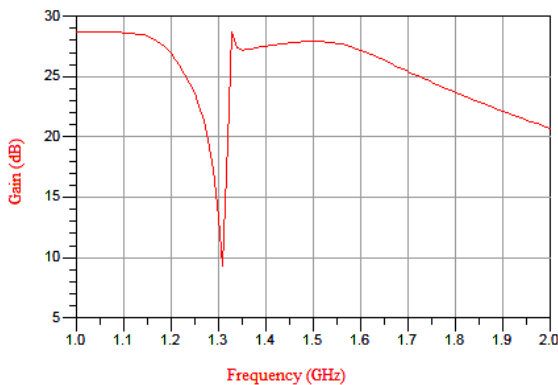


**Fig. 6** Simulation result of gain parameter.

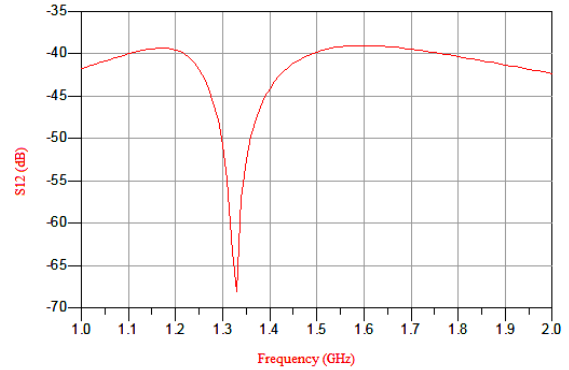


**Fig. 7** Simulation result of S12 parameter.

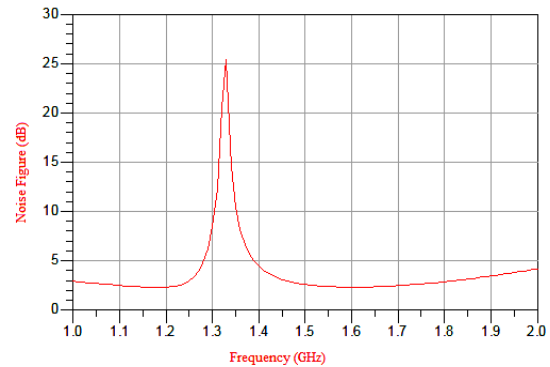


**Fig. 8** Simulation result of NF.

Regarding proper isolation between input and output, NF is only affected by the input matching. Avoiding balun in the input part of LNA is another factor to keep NF minimum.

Fig. 9 presents 1-dB compression point and linearity performance of the proposed LNA.  $P_{-1dB}$ , as shown in Fig. 9, is -15.3 and -13 dBm in 1.2 and 1.57 GHz, respectively. Using differential structure and balancing with compensation capacitor results in even harmonics' attenuation and perfect linearity in LNA's performance.

IIP3 of the designed LNA is presented in Fig. 10. With respect to this figure, its value is -0.9 and 2.2 dBm in 1.2 and 1.57 GHz, respectively. During concurrent operation, linearity is extremely important. Figs. 9 and 10 clearly prove that designed LNA has achieved the desired results in terms of linearity.

To evaluate the stability of the proposed structure, Rollett's parameters [21] are depicted in Figs. 11 and 12 based on the following equations:

$$\begin{cases} K = \frac{1 - |S_{11}|^2 - |S_{22}|^2 + |\Delta|^2}{2|S_{12}S_{21}|} \geq 1 \\ |\Delta| = |S_{11}S_{22} - S_{12}S_{21}| \leq 1 \end{cases} \quad (11)$$

According to Fig. 11, stability constant (K) reaches 10.18 and 12.256 in 1.2 and 1.57 GHz, respectively. Fig. 12 shows that  $|\Delta|$  is about 0.076 and 0.106 in these frequencies. So, it is self-evident that the Rollett's conditions are satisfied and the amplifier is unconditionally stable.

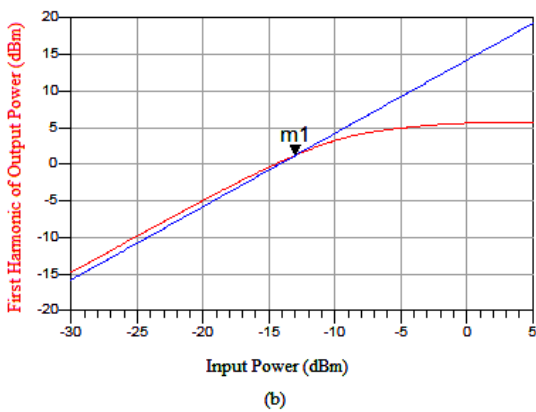
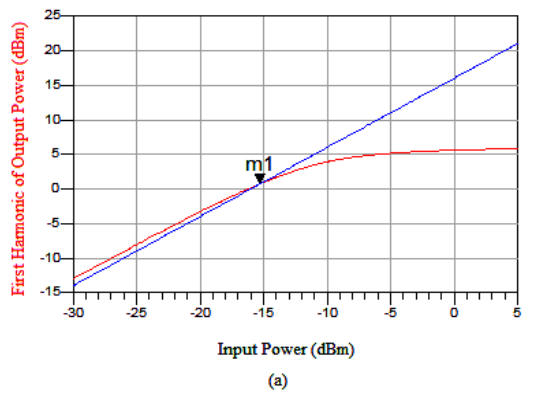


**Fig. 9** Simulation result of P<sub>-1dB</sub> at (a) 1.2 GHz and (b) 1.57 GHz.

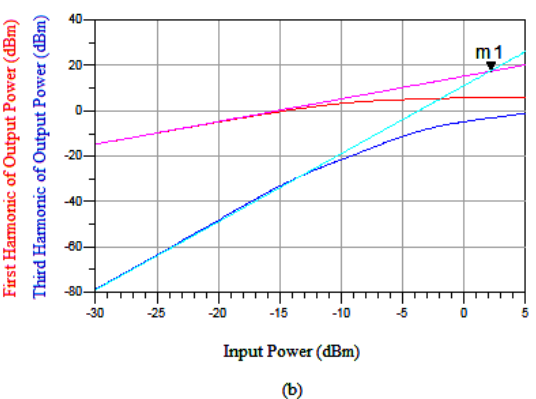
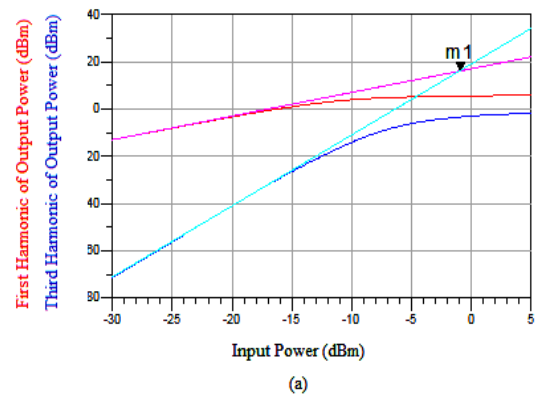


**Fig. 10** Simulation result of IIP<sub>3</sub> at (a) 1.2 GHz and (b) 1.57 GHz.

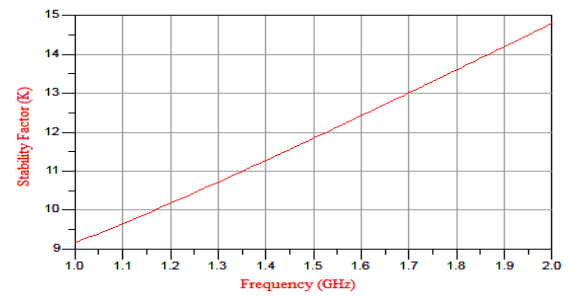


**Fig. 11** Simulation result of stability factor (K).

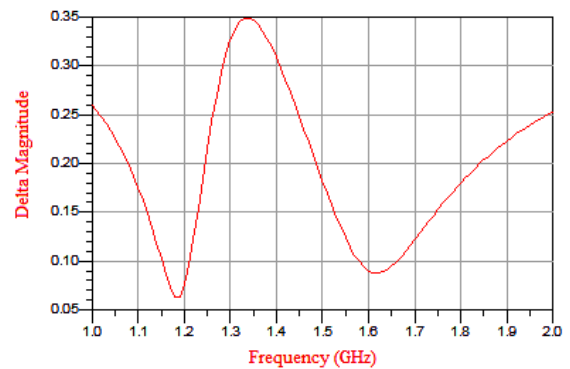


**Fig. 12** Simulation result of delta magnitude.

As shown in the Table 2, a comparative study is carried out between proposed LNA in this paper with previous works. Proposed LNA has concurrent dual-band performance capability. Besides, differential structure has led to a better linearity and increased LNA's gain. Designed LNA has also reached an extremely reasonable amount in input matching and NF simultaneously in both bands.

Also, to show the effectiveness of the proposed structure a Figure Of Merit (FOM) is defined as follow:

$$FOM = \frac{Gain [lin] \cdot f [GHz]}{S11 [lin] \cdot (NF [lin] - 1) \cdot P [mW]} \quad (12)$$

Based on the Eq. (11), it is self-evident that greater value for FOM proves the better performance of circuit.

As can be seen in Table 2, the value of the FOM for the proposed structure is approximately 2.5 times and 8.7 times of FOM in [18] for 1.2 GHz and 1.57 GHz, respectively. Furthermore, the amount of FOM for proposed circuit increased by around 49% compared to FOM in [4] for 1.2 GHz. In comparison with [22], there is not only a reduction of about 46% in power consumption, but also there is a serious difference in FOM value (8.996 compared to 1.343 for 1.2 GHz and 15.97 compared to 2.044 for 1.57 GHz).

#### 4 Conclusion

Concurrent dual-band LNA of a GNSS receiver, which works in two require frequency bands 1.2 GHz and 1.57 GHz, is designed and simulated in this paper.

Simulation results declare that LNA's performance achieves acceptable results in both frequency bands simultaneously.

Results include perfect input matching, gain, NF and linearity. Not only pseudo-differential structure has modified the gain, it also has minimized NF. Furthermore, parallel and series resonance parts have enhanced the input matching capability. As a result proposed LNA can be considered as a perfect choice for concurrent multi-band single-channel GNSS receiver.

## Appendix

The small-signal equivalent circuit of Fig. 1 is demonstrated in Fig. 13.

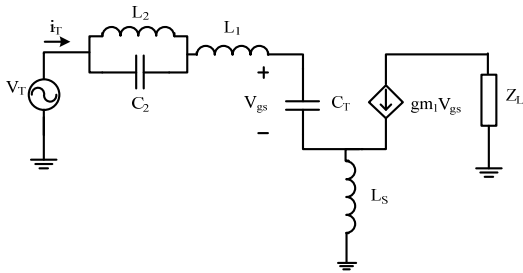


Fig. 13 Small-signal of Fig. 1.

According to Fig. 11, the small-signal input impedance can be calculated by using Eqs. (13) to (18), respectively:

$$\text{KVL: } -V_T + \left[ (jL_2\omega) \left\| \left( \frac{1}{jC_2\omega} \right) + jL_1\omega + \frac{1}{jC_t\omega} \right\| I_T \right] \quad (13)$$

$$+ jL_S\omega (I_T + g_{m1} V_{gs1}) = 0$$

$$(jL_2\omega) \left\| \left( \frac{1}{jC_2\omega} \right) \right\| = \frac{(jL_2\omega) \left( \frac{1}{jC_2\omega} \right)}{(jL_2\omega) + \left( \frac{1}{jC_2\omega} \right)} = \frac{jL_2\omega}{1 - L_2 C_2 \omega^2} \quad (14)$$

$$V_{gs1} = \frac{1}{jC_t\omega} I_T \quad (15)$$

$$V_T = I_T \left[ \frac{jL_2\omega}{1 - L_2 C_2 \omega^2} + jL_1\omega + \frac{1}{jC_t\omega} + jL_S\omega + \frac{jL_S\omega g_{m1}}{jC_t\omega} \right] \quad (16)$$

$$Z_{in} = \frac{V_T}{I_T} \quad (17)$$

$$Z_{in} = \left( \frac{g_{m1} L_S}{C_t} \right) + j\omega \left( \frac{L_2}{1 - \omega^2 L_2 C_2} + L_1 + L_S - \frac{1}{\omega^2 C_t} \right) \quad (18)$$

Table 2 Performance comparison

Parameter	Proposed structure	[18]	[4]	[22]
Process	0.18 $\mu\text{m}$ CMOS	0.18 $\mu\text{m}$ CMOS	0.18 $\mu\text{m}$ CMOS	90 nm CMOS
Structure	Pseudo-differential	Single-ended-to-differential	Pseudo-differential	Differential
Concurrent dual-band	Yes	Yes	No	No
Supply voltage (V)	1.8	1.8	1.8	1
Power consumption (mW)	14.967	11.16	18	28
Frequency (GHz)	1.2/1.57	1.217/1.568	1.2/1.57	1.8/2
S11 (dB)	-11.024/-13.131	-10.6/-10.7	-12/-11	< -10
Gain (dB)	26.926/27.576	13/11.5	23/20	15/16
NF (dB)	2.315/2.333	1.58/3	2.1/2.3	4/3.5
P-1dB (dBm)	-15.3/-13	-14/-13.5	-	-
IIP3 (dBm)	-0.9/2.2	-	-5.7/-3.9	+11
FOM	8.996/15.97	3.619/1.817	6.032/4.431	1.343/2.044

## References

- [1] M. S. Braasch and A. J. Dierendonck, "GPS Receiver Architectures and Measurements", *Proc. IEEE*, Vol. 87, No. 1, pp. 48-64, Jan. 1999.
- [2] M. R. Mosavi, S. Azarshahi, I. Emamgholipour and A. A. Abedi, "Least Squares Techniques for GPS Receivers Positioning Filter using Pseudo-Range and Carrier Phase Measurements", *Iranian Journal of Electrical & Electronic Engineering*, Vol. 10, No. 1, pp. 18-26, 2014.
- [3] M. R. Mosavi and Z. Shokhmzan, "Spoofing Mitigation of GPS Receiver using Least Mean Squares-Based Adaptive Filter", *Iranian Journal of Electrical & Electronic Engineering*, Vol. 11, No. 3, pp. 1-11, 2015.
- [4] D. Chen, W. Pan, P. Jiang, J. Jin, T. Mo and J. Zhou, "Reconfigurable Dual-Channel Multiband RF Receiver for GPS/Galileo/BD-2 Systems", *IEEE Trans. on Microwave Theory and Techniques*, Vol. 60, No. 11, pp. 3491-3501, Nov. 2012.
- [5] D. Margaria, F. Dosis and P. Mulassano, "An Innovative Data Demodulation Technique for Galileo AltBOC Receivers", *Journal of Global Positioning Systems*, Vol. 6, No. 1, pp. 89-96, 2007.
- [6] C. F. Prades, L. L. Presti and E. Falletti, "Satellite Radio Localization from GPS to GNSS and Beyond: Novel Technologies and Applications

- for Civil Mass Market”, *Proc. IEEE*, Vol. 99, No. 11, pp. 1882-1904, Nov. 2011.
- [7] J. F. Chang and Y. S. Lin, “0.99 mW 3-10 GHz Common Gate CMOS UWB LNA using T-Match Input Network and Selfbody-Bias Technique”, *Electronics Letters*, Vol. 47, No. 11, pp. 658-659, May 2011.
- [8] G. Sapone and G. Palmisano, “A 3-10 GHz Low-Power CMOS Low-Noise Amplifier for Ultra-Wideband Communication”, *IEEE Trans. on Microwave Theory and Techniques*, Vol. 59, No. 3, pp. 678-686, March 2011.
- [9] S. Arshad, F. Zafar, R. Ramzan and Q. Wahab, “Wideband and Multiband CMOS LNAs: State-of-the-Art and Future Prospects”, *Journal of NED University of Engineering & Technology*, Vol. 44, pp. 774-786, Sept. 2013.
- [10] J. Ko, J. Kim, S. Cho and K. Lee, “A 19-mW 2.6-mm<sup>2</sup> L1/L2 Dual-Band CMOS GPS Receiver”, *IEEE Journal of Solid-State Circuits*, Vol. 40, No. 7, pp. 1414-1425, July 2005.
- [11] N. Qi, Y. Xu, B. Chi, X. Yu, X. Zhang, N. Xu, P. Chiang, W. Rhee and Z. Wang, “A Dual-Channel Compass/ GPS/ GLONASS/ Galileo Reconfigurable GNSS Receiver in 65 nm CMOS with On-Chip I/Q Calibration”, *IEEE Trans. on Circuits and Systems I: Regular Papers*, Vol. 59, No. 8, pp. 1720-1732, Aug. 2012.
- [12] J. Wu, P. Jiang, D. Chen and J. Zhou, “A Dual-Band GNSS RF Front End with a Pseudo-Differential LNA”, *IEEE Trans. on Circuits and Systems*, Vol. 58, No. 3, pp. 134-138, March 2011.
- [13] D. Chen, T. Yan, J. Jin, C. Mao, Y. Lu, W. Pan and J. Zhou, “A Tri-Mode COMPASS/GPS/Galileo RF Receiver with All-Digital Automatic Gain Control Loop”, *Analog Integrated Circuits Signal Processing*, Vol. 70, No. 1, pp. 69-77, Jan. 2012.
- [14] M. Detratti, E. López, E. Pérez, R. Palacio and M. Lobeira, “Dual-Band RF Receiver Chip-Set for Galileo/GPS Applications”, *IEEE Symposium on Location and Navigation*, pp. 851-859, May 2008.
- [15] D. Chen, W. Pan, P. Jiang, J. Jin, T. Mo and J. Zhou, “Reconfigurable Dual-Channel Multiband RF Receiver for GPS/Galileo/BD-2 Systems”, *IEEE Trans. on Microwave Theory and Techniques*, Vol. 60, No. 11, pp. 3491-3501, Nov. 2012.
- [16] M. Conta, E. Rodal, S. Anand, H. Jensen, H. Huang, Y. W. Lin, Z. Liu, F. D. Flaviis and K. Benboudjema, “A 0.9 dB NF 9 mW 28 nm Triple-Band GNSS Radio Receiver”, *IEEE Conference on Radio Frequency Integrated Circuits Symposium*, pp. 213-216, June 2014.
- [17] I. Jo, J. Bae, T. Matsuoka and T. Ebinuma, “RF Front-End Architecture for a Triple-Band CMOS GPS Receiver”, *Journal on Microelectronics*, Vol. 46, pp. 27-35, Jan. 2015.
- [18] J. Shen and X. Zhang, “Concurrent Dual-band LNA for Dual-system Dual-band GNSS Receiver”, *Analog Integrated Circuits Signal Processing*, Vol. 78, No. 2, pp. 529-537, 2014.
- [19] H. Hashemi and A. Hajimiri, “Concurrent Multiband Low-Noise Amplifiers-Theory, Design, and Applications”, *IEEE Trans. on Microwave Theory and Techniques*, Vol. 50, No. 1, pp. 288-301, Jan. 2002.
- [20] T. K. Nguyen, C. H. Kim, G. J. Ihm, M. S. Yang and S. G. Lee, “CMOS Low-Noise Amplifier Design Optimization Techniques”, *IEEE Transactions on Microwave Theory and Techniques*, Vol. 52, No. 5, pp. 1433-1442, May 2004.
- [21] G. Gonzalez, *Microwave Transistor Amplifiers Analysis and Design*, 2<sup>nd</sup> Edition, Chapter 3, Prentice-Hall, 1984.
- [22] G. Z. Fatin, Z. D. Koozehkanani and H. Sjoland, “A 90 nm CMOS +11 dBm IIP3 4 mW Dual-Band LNA for Cellular Handsets”, *IEEE Microwave and Wireless Components Letters*, Vol. 20, No. 9, pp. 513-515, Sept. 2010.



**Maryam Safari** received her B.Sc. and M.Sc degrees in Electronic Engineering from Babol Noshirvani University of Technology in 2009 and University of Zanjan in 2012, respectively. She is currently a Ph.D. student in the Department of Electrical Engineering at Iran University of Science and Technology. Her research interests include analog integrated circuit design, RF microelectronics and global positioning systems.



**Minoos Eghtesadi** received her B.Sc. degree in Electronic Engineering from Khajeh Nasir Toosi University of Technology, Tehran, Iran in 2013. She is currently a M.Sc. student in Iran University of Science and Technology in Electronic Engineering, Tehran, Iran. Her research interests include analog integrated circuit design.



**Mohammad-Reza Mosavi** received his B.Sc., M.Sc., and Ph.D. degrees in Electronic Engineering from Iran University of Science and Technology (IUST), Tehran, Iran in 1997, 1998, and 2004, respectively. He is currently faculty member of Department of Electrical Engineering of IUST as professor. He is the author of more than 260 scientific publications on journals and international conferences. His research interests include circuits and systems design.